24th COBEM - 2017

24th ABCM International Congress of Mechanical Engineering
December 3-8, 2017, Curitiba, PR, Brazil

COBEM-2017-1912
EXPERIMENTAL ANALYSIS OF AN ENERGY HARVESTING SYSTEM WITH PIEZOELECTRIC AND SHAPE MEMORY ALLOY

Arthur Adeodato
CEFET/RJ, Programa de Pós-Graduação em Engenharia Mecânica e Tecnologia de Materiais (PPEMM), Rio de Janeiro, RJ, Brasil
adeodatoarthur@hotmail.com

Brenno Tavares Duarte
CEFET/RJ, Programa de Pós-Graduação em Engenharia Mecânica e Tecnologia de Materiais (PPEMM), Rio de Janeiro, RJ, Brasil
brenno_duarte@yahoo.com

Ricardo Alexandre Amar de Aguiar
CEFET/RJ, Programa de Pós-Graduação em Engenharia Mecânica e Tecnologia de Materiais (PPEMM), Rio de Janeiro, RJ, Brasil
ricardoamar@yahoo.com

Luciana Loureiro da Silva Monteiro
CEFET/RJ, Programa de Pós-Graduação em Engenharia Mecânica e Tecnologia de Materiais (PPEMM), Rio de Janeiro, RJ, Brasil
lucianals@lts.coppe.ufrj.br

Marcelo Amorim Savi
COPPE/UFRJ, Programa de Pós-Graduação em Engenharia Mecânica (PEM), Rio de Janeiro, RJ, Brazil
savi@mecanica.coppe.ufrj.br

Pedro Manuel Calas Lopes Pacheco
CEFET/RJ, Programa de Pós-Graduação em Engenharia Mecânica e Tecnologia de Materiais (PPEMM), Rio de Janeiro, RJ, Brasil
pedro.pacheco@cefet-rj.br

Abstract. *Conversion of environmental mechanical vibrations into electrical power has attracted the attention of several researchers, introducing the concept of energy harvesting by using piezoelectric materials. Optimal operational conditions for energy harvesting devices using piezoelectric elements occurs when the system external excitation is close to it resonance frequency. Large reduction of generated power can occur outside of this condition, and the use of adaptive device strategies is an interesting approach. As the environmental sources usually operate within a range of vibration frequencies, the synergic effect of piezoelectric materials and shape memory alloys (SMA) can be used to increase the operating range of the system by using the pseudoelastic and shape memory alloy effects. SMAs hysteretic effects and material elastic modulus variations associated to phase transformations introduces changes in the damping and stiffness characteristics of the SMA element. These changes affect the system dynamic allowing the tuning of the system with the excitation frequencies. This work deals with an experimental analysis of a piezoelectric cantilever beam coupled with a shape memory alloy helical spring excited by a shaker considering different vibration conditions and temperatures. Experimental results show that the proposed device configuration can be used to extend the operational range of the device for variable vibration excitation conditions.*

Keywords: *Energy Harvesting, Piezoelectric Material, Shape Memory Alloy, Experimental Analysis*

1. INTRODUCTION

Over the last fifteen years, the term energy harvesting has been explored in many works and used to express the process of convert mechanical energy available on the nature into electrical power. One of the most studied alternative to energy harvesting is about piezoelectric materials submitted to mechanical vibrations. Piezoelectric materials present electromechanical coupling, it means, when submitted to a mechanical loading, an electrical polarization is induced and it is proportional to applied mechanical stress (direct effect), also exhibit the converse piezoelectric effect (the generation of stress when an electric field is applied). The vast majority of literature addresses linear electrical-mechanical conversion approaches for energy harvesting with piezoelectric material (Inman *et al.*, 2005; Sodano and

Inman, 2007; Choock-Chennault *et al.*, 2008; Erturk and Inman, 2011). A common energy harvesting device uses a cantilever beam with a tip mass and piezoelectric patches excited in the transverse direction at its base using harmonic or stochastic forces. Once the natural frequency is tuned to the excitation frequency the system has a maximum output power, resulting in a narrowband harvester system. Several researchers have been worked to enhance the frequency response of the energy harvester introducing different nonlinearities into the system. The possibility of transform the energy harvester in a broadband system can be achieved by different methods: using bistable structures (Erturk and Inman, 2011), using mechanical preload (Leland and Wright, 2006), including asymmetric tip mass (Bai et al., 2014), varying the geometry of the structural energy harvester (Hu et al., 2007; Friswell et al., 2012), including mechanical end-stops (Basset et al., 2014).

Many researches have dedicated their time trying to extend the operational range of piezoelectric devices making then more efficient, exploring nonlinearities added to the system (Erturk et al., 2009; Nguyen *et al.*, 2013; Bai *et al.*, 2014).

Another way to include nonlinearities into the system is the synergistic use of smart materials. The inclusion of shape memory alloys (SMAs) elements can enhance energy harvesting performance. SMAs present martensitic phase transformation that can be exploited either to change stiffness or to dissipated energy (Monteiro *et al.*, 2015). The main objective of this article is to experimentally study the behavior of a piezoelectric energy harvester coupled to a SMA element. SMAs comes up as an alternative to make piezoelectric devices for energy harvesting more applicable when submitted to a range of different frequencies. This other type of smart material presents thermomechanical coupling and two main effects named shape memory effect and pseudoelasticity, both associated to phase transformation promoted by mechanical or thermal loads. Two phases are present and have different elastic modulus values. Austenite is stable at high temperatures and have the higher elastic modulus value. Martensite is stable at low temperatures. Hysteretic effect is also present during phase transformation. These two effects can be used to change the stiffness and damping characteristics of the system (Lagoudas, 2008; de Aguiar *et al.*, 2012). Figure 1 shows a *Stress x Strain* diagram for a SMA material representing the shape memory (a) and pseudoelastic effect (b). In Fig. 1 (a), σ_s and σ_f, represent the start and final critical stresses for the mechanical loading reorientation process. Residual strain can be recovered with the application of a thermal load (from point E to F). A_s and A_f represent the start and final temperature for austenite phase formation during a thermal load. In Fig. 1 (b), σ^{MS}, σ^{MF}, σ^{AS} and σ^{AF} represent the critical stresses for the phase transformation induced by mechanical load in a pseudoelastic behavior. The area under the curves in Fig. 1 (b) represents the energy absorbed during a load and unload process.

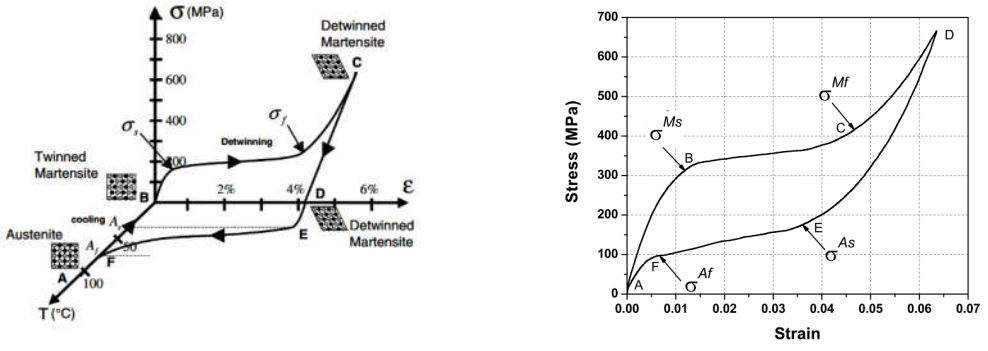

(a) (b)

Figure 1 – Stress x Strain diagram for Shape memory effect (a) and Pseudoelastic effect (b). (LAGOUDAS, 2008)

This paper deals with the synergistic use of smart materials for energy harvesting purposes. In essence, piezoelectric and shape memory alloys are combined to build an energy harvesting system. On this way, an experimental apparatus was developed containing a piezoelectric energy harvester element coupled to SMA helical springs. The system was submitted to different vibration amplitudes and temperature conditions. Experimental results show that the synergetic use of piezoelectric material and shape memory alloys can increase the operational range of energy harvester devices.

2. EXPERIMENTAL PROCEDURE

To analyse the behaviour of a piezoelectric energy harvester, a prototype made of an aluminium cantilever beam with a piezoelectric element coupled to the aluminium beam was used. The piezoelectric element used was provided by *Piezo Systems* and it is a *Q220-A4-503YB* model. Table 1 deals with the piezoelectric and aluminium beam dimensions.

Table 1 – Piezoelectric element and aluminium beam dimensions

Dimensions / Component	Piezoelectric Element	Aluminum Beam
Length (mm)	63.5	135
Width (mm)	31.8	60
Thickness (mm)	0.51	2

A mechanical excitation is applied to one of the ends of the beam by an electromechanically shaker V350 from Data Physics. Lasers transducers, *optonNCDT 2200* from *Micro-Epsilon (με),* were used to measure the displacement of the base (exited by the shaker) and the other end of the beam. A data acquisition system (*Spider 600 Hz model from HBM*) was used to capture the transducer signals.

A SMA helical spring presenting shape memory effect and another presenting pseudoelastic effect at room temperature (24 ºC) were connected to the beam end opposite to the base end. Before starting vibration tests with energy harvester system, thermal-mechanical characterization of SMA springs have to be performed though a differential Scanning Calorimeter (DSC) where it is possible to identify the phase transformation temperatures and tensile tests using a test machine Instron to obtain the mechanical characterization at room temperature. Figure 2 shows *Force x Displacement* diagrams for both SMA springs obtained from tensile tests developed in a *Instron 5966*. Table 2 specifies some mechanicals and geometrical properties for the used springs. M_s and M_f represents the start and final martensite temperature transformation and A_s and A_f austenite temperature transformation, respectively. A pre-extension was applied in the SMA springs to guarantee that the spring would be submitted only to tensile stresses and avoid nonlinear effects provided by non-smooth vibration movement. Figure 3 shows the vibration experimental apparatus mount and its main components.

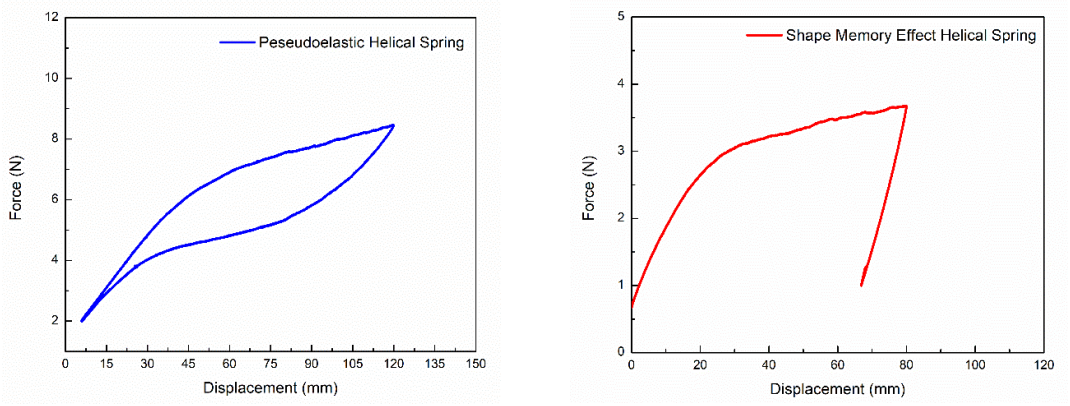

(a) (b)

Figure 2 – *Force x Displacement* diagram for a tensile test (a) Peseudoelastic Effect used spring and (b) Shape Memory Effect used spring.

Table 2 – Mechanical and geometrical SMA used springs

Property	Pseudoelastic Helical Spring	Shape Memory Alloy Helical Spring
Beginning Stiffness (N/m)	117	110
Wire Diameter (mm)	0.9	0.8
Spring Diameter (mm)	12	5.6
Pre-extension (mm)	42	25
Number of active spires	10	45
M_f °C	-10.35	31.75
M_s °C	1.1	41.65
A_s °C	-4.05	26.10
A_f °C	20.45	50.04

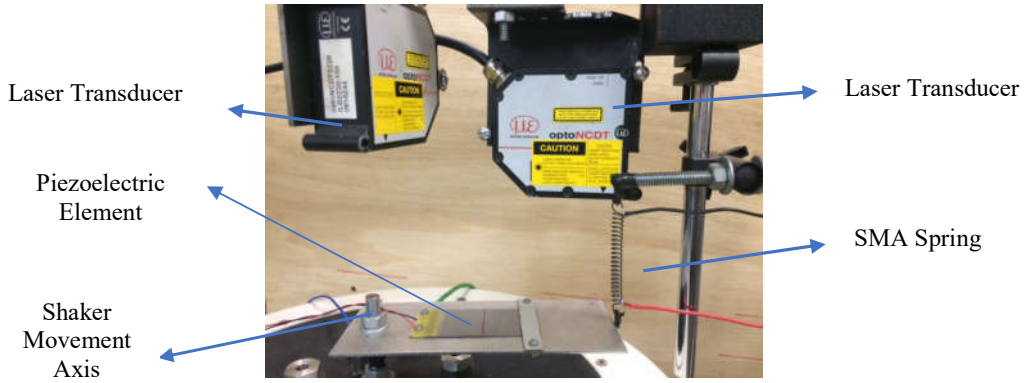

Figure 3 – Experimental apparatus and its main components.

The base acceleration amplitudes of 6 m/s² and 9.8 m/s² were considered. Both SMA springs were heated by Joule's Effect for 4 conditions: zero-current (0 A) and 0.5, 1.0 and 1.5 A. Tests were performed considering that the SMA spring was coupled to the harvester system, free of stress and current. A pre-extension was first applied to the spring. A prescribed constant amplitude base acceleration was then applied with the frequency varying from 65 Hz to 75 Hz. To guarantee the consistency of the results, all tests were done 3 times for the same condition. After performed 3 times for the condition 0 A, the SMA spring was removed from the system and heated with 1.0 A for 60 seconds which allows to homogenize the microstructure of SMA material. An interval of 5 minutes was adopted for spring cooling by natural convection. Again, the SMA spring was coupled to the system and performed three new tests for the condition of 0.5 A. The process was repeated for the 4 conditions, resulting in 48 tests.

3. RESULTS AND DISCUSSIONS

Results shows that for each different temperature associated to different electrical currents the system presents response variation associated to damping and stiffness variation carrying different values for resonance.

Figure 4 and 5 shows the frequency response of the system coupled to a pseudoelastic helical spring submitted to base vibrations of 6 m/s² and 9.8 m/s², respectively. Results show that for a condition where the pseudoelastic spring has predominant austenite phase, an increase in temperature would not be able to make significant changes to resonance frequency that could occur as a result of the system stiffness variation. A small peak reduction is observed and can be associated to the rise of the dissipation. Dissipation experiences a little increase according to the temperature reaching a maximum value once the shape memory element would be working in a high temperature and only on the linear-elastic phase (no more dissipation). Tables 3 and 5 presents the maximum average values measured for electrical tension and the value for respective resonance condition. Tables 4 and 6 presents the maximum average values measured for tip displacement and the value for respective resonance condition. All then also presents the standard deviation and error calculated by the *Origin Pro 8.5* software.

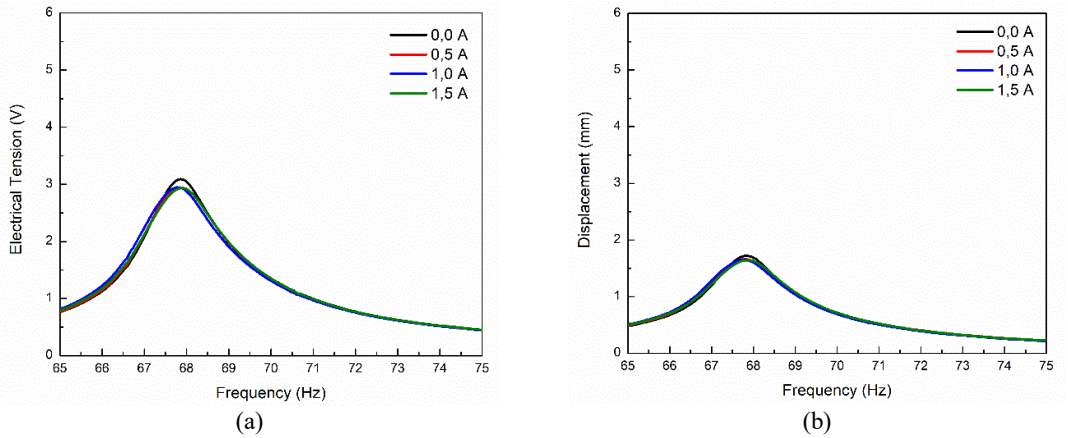

(a) (b)

Figure 4 – Electrical tension amplitude x oscillation frequency (a). Tip displacement x oscillation frequency (b). Base acceleration of 6 m/s². Pseudoelastic spring coupled.

Table 3 – Electrical tension measured on the top point of resonance – 6 m/s².

Electrical Current (A)	Resonance Frequency (Hz)	Electrical Tension (V)	Standard Deviation (V)	Error
0.0	67.854	3.089	0.019	0.011
0.5	67.840	2.944	0.004	0.002
1.0	67.786	2.945	0.003	0.001
1.5	67.908	2.933	0.023	0.013

Table 4 – Tip displacement measured on the top point of resonance – 6 m/s².

Electrical Current (A)	Resonance Frequency (Hz)	Tip Displacement (mm)	Standard Deviation (mm)	Error
0.0	67.832	1.719	0.004	0.002
0.5	67.799	1.661	0.002	0.001
1.0	67.744	1.477	0.017	0.010
1.5	67.847	1.642	0.010	0.005

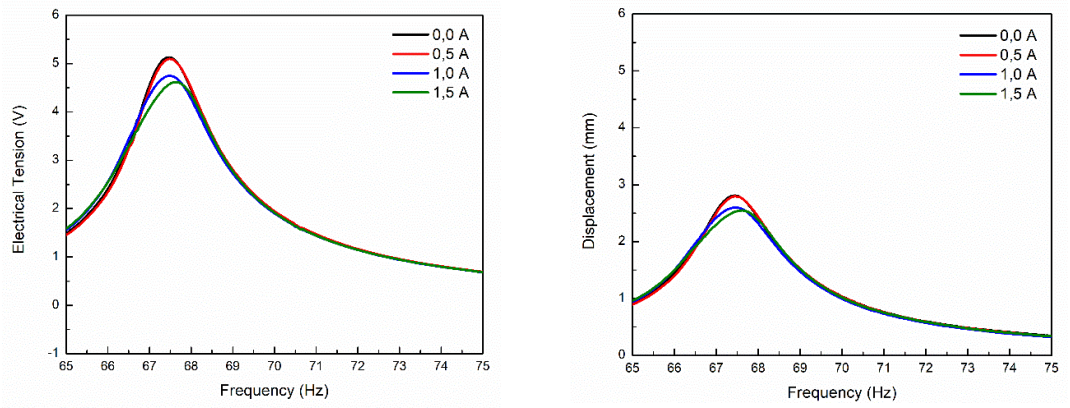

(a) (b)

Figure 5 – Electrical tension amplitude x oscillation frequency (a). Tip displacement x oscillation frequency (b). Base acceleration of 9.8 m/s². Pseudoelastic spring coupled.

Table 5 – Electrical tension measured on the top point of resonance - 9,8 m/s².

Electrical Current (A)	Resonance Frequency (Hz)	Electrical Tension (V)	Standard Deviation (V)	Error
0.0	67.462	5.129	0.030	0.017
0.5	67.524	5.090	0.017	0.010
1.0	67.482	4.750	0.130	0.075
1.5	67.647	4.618	0.002	0.001

Table 6 – Tip displacement measured on the top point of resonance – 6 m/s².

Electrical Current (A)	Resonance Frequency (Hz)	Tip Displacement (mm)	Standard Deviation (mm)	Error
0.0	67.421	2.808	0.012	0.007
0.5	67.482	2.790	0.011	0.006
1.0	67.462	2.601	0.071	0.041
1.5	67.647	2.547	0.004	0.003

A new approach is on focus now. Figure 6 and 7 presents the results obtained with base vibrations prescribed amplitudes of 6 m/s² and 9.8 m/s² now with a shape memory effect helical spring coupled to the energy harvesting system.

Under this condition, stress-induced phase transformation occurs and therefore, two effects affect the dynamical behavior of the system: SMA element stiffness variation promoted by the dependence of the Young modulus on the volume fraction phase; and the dissipation associated with the hysteretic behavior. On this reason, the resonance frequency on the curves presented on Fig. 6 and 7 takes different values and some of them providing even more electrical tension and tip displacement than with the SMA spring in ambient temperature. The resonance frequency shift to the right (larger values) for larger electric current values (and, as consequence, larger temperature values) is associated to the effect of stiffness rise promoted by the presence of austenite phase that have a larger elastic modulus.

In Fig. 7, for 0.5 A the curve takes a lower resonance value compared to a 0 A condition and stars to increase after 1.0 A presenting a nonlinear effect associated to the SMA behavior.

Results show that by controlling the electric current, the operational range of the system can be extended and are in agree with numerical simulations from previews works (Monteiro *et al.*, 2015).

Tables 7 and 9 presents the maximum average values measured for electrical tension and the value for respective resonance condition. Tables 8 and 10 presents the maximum average values measured for tip displacement and the value for respective resonance condition. All then also presents the standard deviation and error calculated by the *Origin Pro 8.5* software.

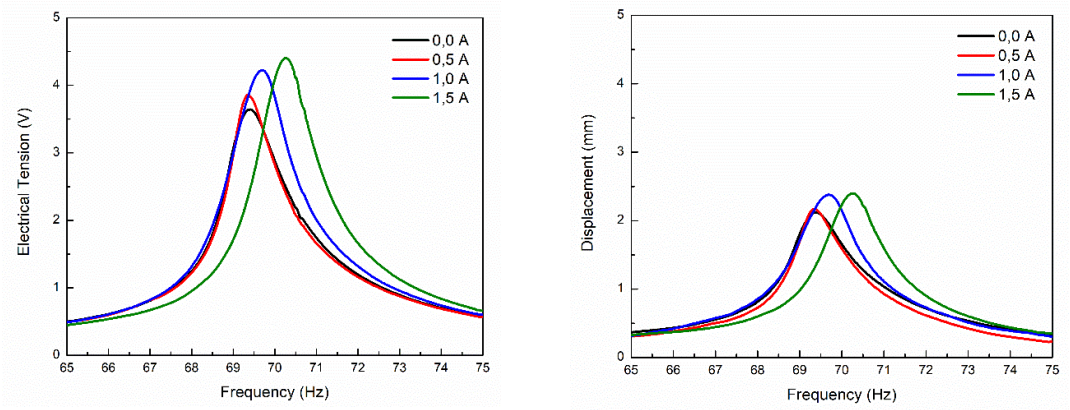

(a) (b)

Figure 6 – Electrical tension amplitude x oscillation frequency (a). Tip displacement x oscillation frequency (b) Base amplitude acceleration of 6 m/s². SME spring coupled.

Table 7 – Electrical tension measured on the top point of resonance - 6 m/s².

Electrical Current (A)	Resonance Frequency (Hz)	Electrical Tension (V)	Standard Deviation (V)	Error
0.0	69.409	3.642	0.032	0.018
0.5	69.334	3.858	0.039	0.023
1.0	69.697	4.224	0.019	0.011
1.5	70.268	4.405	0.014	0.008

Table 8 – Tip displacement measured on the top point of resonance – 6 m/s².

Electrical Current (A)	Resonance Frequency (Hz)	Tip Displacement (mm)	Standard Deviation (mm)	Error
0.0	69.409	2.117	0.013	0.007
0.5	69.354	2.170	0.063	0.036
1.0	69.677	2.379	0.050	0.028
1.5	70.248	2.398	0.031	0.018

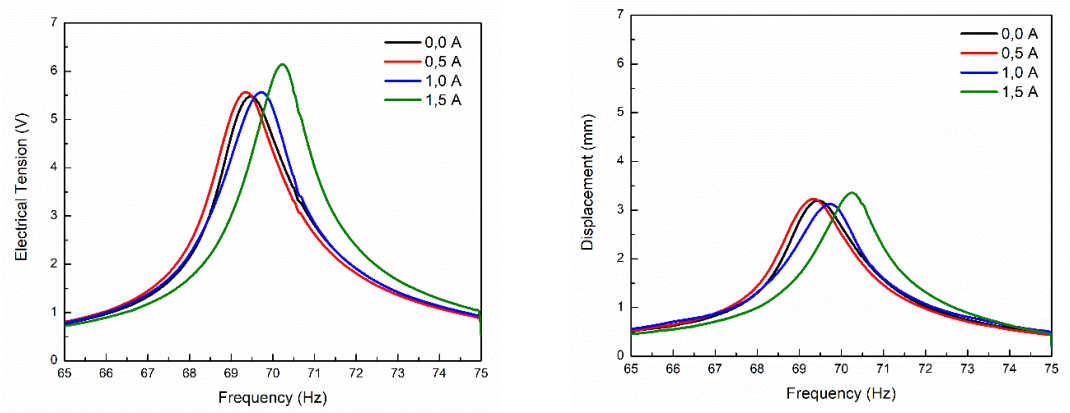

(a) (b)

Figure 7 – Electrical tension amplitude x oscillation frequency (a). Tip displacement x oscillation frequency (b) Base amplitude acceleration of 9.8 m/s². SME spring coupled.

Table 9 – Electrical tension measured on the top point of resonance – 9.8 m/s².

Electrical Current (A)	Resonance Frequency (Hz)	Electrical Tension (V)	Standard Deviation (V)	Error
0.0	69.460	5.479	0.008	0.005
0.5	69.347	5.568	0.010	0.006
1.0	69.717	5.563	0.019	0.011
1.5	70.227	6.138	0.027	0.016

Table 10 – Tip displacement measured on the top point of resonance – 9.8 m/s².

Electrical Current (A)	Resonance Frequency (Hz)	Tip Displacement (mm)	Standard Deviation (mm)	Error
0.0	69.460	3.194	0.001	0.001
0.5	69.326	3.226	0.006	0.003
1.0	69.737	3.124	0.046	0.026
1.5	70.247	3.354	0.007	0.004

Comparing the results obtained for a traditional piezoelectric energy harvester system (piezoelectric coupled to the aluminum beam) and the system coupled to a shape memory effect spring varying its temperature as described in this paper, the reader can observe a strongly difference between both conditions. Figure 8 (a) show that for a force frequency condition of 70,25 Hz (for example, in this case), the system whit shape memory effect spring coupled can be tuned for a better performance, heating the SMA element. In Fig. 8 (b), one can see the bandwidth for both cases. As a criterion, was taken 50% of the total electrical tension obtained in each case. Was defined as Δf_L and Δf_{NL} the bandwidth for a linear system (traditional piezoelectric energy harvester) and nonlinear system (coupled to the SMA spring) respectively. From Fig. 8 (b) its observed that Δf_L = 1,905 and Δf_{NL} = 2,850 showing that the bandwidth can be extended using a SMA spring summited to different temperatures.

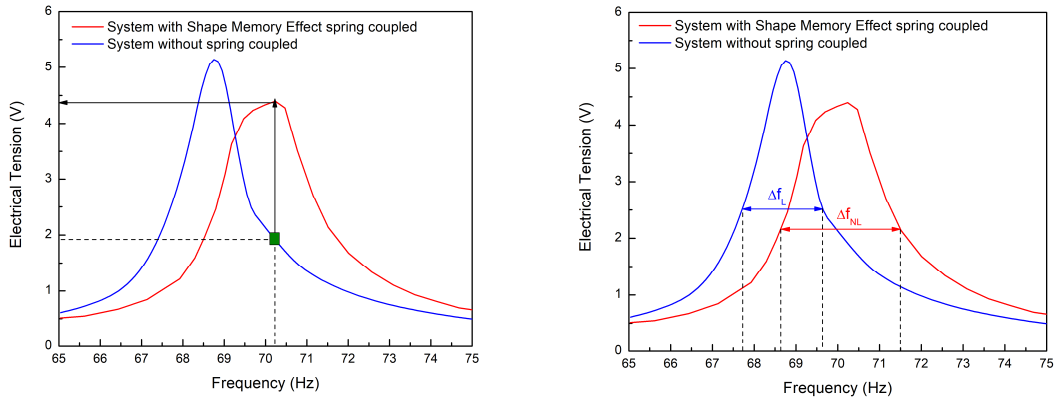

Figure 8 – Comparing traditional piezoelectric energy harvester with piezoelectric energy harvester coupled to a shape memory effect spring for different temperatures. In case of a control system implemented (a). Extended bandwidth (b). Base amplitude acceleration of 6 m/s².

4. CONCLUSIONS

Since ambient vibrations can be frequency-varying or totally random with energy distributed over a wide frequency range, the development of adaptive energy harvester devices seams an interesting and complex field to be explored. The main idea is to use temperature variations to enhance energy harvesting. Experimental tests are carried out at different temperatures and motion amplitudes showing distinct responses of the system. Basically, it is possible to change the generated power amplitude and also, to shift the peak of the power curve as a function of frequency. A piezoelectric energy harvesting prototype system coupled with a SMA helical spring was used to study the coupled dynamic behavior. Results using pseudoelastic spring show that the voltage peak values are quite similar and the shift on frequency almost disappears using different electrical currents. On the other hand, results show a good potential to extend the system operational range by exploring the shape memory effect associated to phase transformation. Electrical tension amplitude tends to increase and shift the system's resonance frequency. Good agreement is observed with numerical results obtained from previous works of the authors.

5. ACKNOWLEDGMENTS

The authors would like to acknowledge the support of the Brazilian Research Agencies CNPq and CAPES.

6. REFERENCES

Aguiar, R.A.A. de, Savi, M.A., Pacheco, P.M.C.L, 2012. "Experimental investigation of vibration reduction using shape memory alloys". Journal of Intelligent Material Systems. 24,2 (2013): 247-261

Bai, Y., Meggs, C., Button, T. W., 2014. "Investigation of using free-standing thick-film piezoelectric energy harvesters to develop wideband devices" International Journal of Structures Stability and Dynamics 14.08 (2014): 1440016

Basset, P., Galayko, D., Cottone, F., et al., 2014, "Electrostatic vibration energy harvester with combined effect of electrical nonlinearities and Mechanical impact". Journal of Micromechanics and Microengineering, Vol. 24.3: 035001.

Cook-Chennault, K. A., Thambi, N., Sastry, A.M., 2008. "Powering MEMS portable devices—a review of non-regenerative and regenerative power supply systems with special emphasis on piezoelectric energy harvesting systems. Smart Material and Structure. 2008, p. 17 (2008) 043001 (33pp).

Erturk, A., Hoffman, J., Inamn, D.J., 2009. "A piezomagnetoelastic structure for boardband vibration energy harvesting". Applied Physics Letters 94.25 (2009): 254102

Erturk, Alper and Inman, Daniel J., 2011. "Piezoelectric Energy Harvesting". John Wiley & Sons.

Friswell, M.I., Ali, S.F., Adhikari, S., Lees, A.W., Bilgen, O. and Litak, G., 2012, "Nonlinear piezoelectric vibration energy harvesting from a vertical cantilever beam with tip mass", Journal of Intelligent Material Systems and Structures, Vol. 23: 1505-1521.

Hu, H.P., Cui, Z.J. and Cao, J.G., 2007, "Performance of a piezoelectric bimorph harvester with variable width", J Mech Vol. 23.03:197–202.

Inman, D.J., Sodano, H.A., Park, G., 2005. "Comparison of Piezoelectric Energy Harvesting Devices for Recharging Batteries". Journal of Intelligent Material and Structures 16.10 (2005): 799-807.

Lagoudas, Dimitris C., 2008. "Shape Memory Alloys Modeling and Engineering Applications". Springer Science & Business Media, 2008.

Leland, E.S. and Wright, P.K. 2006. ''Resonance Tuning of Piezoelectric Vibration Energy Scavenging Generators Using Compressive Axial Preload,'' Smart Materials Structures, Vol.15:14131420.

Nguyen, S.D., Halvorsen, E., Paprotny, I., 2013. "Bistable springs for wideband microelectromechanical energy harvesters" Applied Physics Letters 102.2 (2013): 023904.

Silva, L.L.M, Oliveira, S.A., Pacheco, P.M.C.L., Savi, M.A., 2015. "Synergistic use of smart materials for vibration-based energy harvesting". The european physical journal special topics. 2015.

Sodano, H.A., Inman, D.J., 2007. "A Review of Power Harvesting from Vibration using Piezoelectric Materials (2003 - 2006)". Smart Materials and Structures. 2007, Vol. v.36(3), p.197-205.

7. RESPONSIBILITY NOTICE

The author(s) is (are) the only responsible for the printed material included in this paper.